Analyst

Handheld biofluorometric system for acetone in the exhaled breath condensates

Journal:	*Analyst*
Manuscript ID	AN-ART-10-2024-001281.R2
Article Type:	Paper
Date Submitted by the Author:	16-Dec-2024
Complete List of Authors:	Zhang, Geng; Institute of Science Tokyo, Graduate School of Medical and Dental Sciences Ichikawa, Kenta; Institute of Science Tokyo, Department of Biomedical Devices and Instrumentation Iitani, Kenta; Institute of Science Tokyo, Department of Biomedical Devices and Instrumentation Iwasaki, Yasuhiko; Kansai University, Department of Chemistry and Materials Engineering Mitsubayashi, Kohji; Institute of Science Tokyo, Department of Biomedical Devices and Instrumentation

Title:

Handheld biofluorometric system for acetone in the exhaled breath condensates

Authors and affiliation

Geng Zhang[a], Kenta Ichikawa[b], Kenta Iitani[b], Yasuhiko Iwasaki[c], Kohji Mitsubayashi[a,b,*]

[a] *Graduate School of Medical and Dental Sciences, Institute of Science Tokyo, 1-5-45 Yushima, Bunkyo-ku, Tokyo 113-8510, Japan*

[b] *Department of Biomedical Devices and Instrumentation, Laboratory for Biomaterials and Bioengineering, Institute of Integrated Research, Institute of Science Tokyo, 2-3-10 Kanda-Surugadai, Chiyoda-ku, Tokyo 101-0062, Japan*

[c] *Faculty of Chemistry, Materials and Bioengineering, Kansai University, Osaka 564–8680, Japan*

** Corresponding author:*

E-mail: m.bdi@tmd.ac.jp

Abstract:

As a marker of human metabolism, acetone is important for lipid metabolism monitoring and early detection of diabetes. In this study, we developed a handheld acetone biosensor based on fluorescence detection by utilizing the enzymatic reaction of secondary alcohol dehydrogenase (S-ADH) with β-nicotinamide adenine dinucleotide (NADH, λex = 340 nm, λem = 490 nm). In the reaction, NADH is oxidized when acetone is reduced to 2-propanol by S-ADH, and acetone concentration can be measured by detecting the amount of NADH consumed in this reaction. First, we constructed the compact and light weight fluorometric NADH detection system (209 g for the sensing system and 342 g for PC) which worked with battery. Then, sensor characteristics were evaluated after optimization of working conditions. The developed system was able to quantify the acetone at a range of 510 nM to 1 mM within 1 minute. The developed battery-operated acetone biosensor demonstrated its ability to measure acetone concentration in exhaled breath condensate of 10 healthy subjects at rest (23.4±15.1 μM) and 16 h of fasting (37.7±14.7 μM) and distinguish with significant differences (p = 0.011). With the advantages of handholdable, high sensitivity and selectivity, this sensor is expected to be widely used in clinical diagnosis and wearable biochemical sensors in the future.

Keywords:

handheld, biosensor, acetone, exhaled breath condensates, fluorescence, fiber-optics

Introduction

Diabetes mellitus (DM) represents a prevalent chronic metabolic disorder primarily characterized by persistent hyperglycemia, with cardiovascular disease, renal failure, and neuropathy all being possible consequences of this disease. It is projected that 578 million people will have diabetes by 2030 and close to half of all diabetics do not know they have diabetes[1, 2], making early detection and timely diagnosis of diabetes very important. Currently, diabetes is mainly diagnosed by measuring blood glucose levels, but this method requires taking the patient's blood, which can cause pain and a certain psychological burden on the patient[3].

Acetone is a metabolite of fat breakdown in the body. The three ketone bodies, acetone, beta-hydroxybutyric acid, and acetoacetic acid, can be found in blood, urine, and exhaled breath. The biochemical pathways and principles of acetone production are well understood[4]. In diabetic patients, insufficient insulin secretion or the presence of insulin resistance leads to abnormal fatty acid metabolisms. As a result, the liver produces excessive ketone bodies, including acetone. Therefore, the concentration of acetone in diabetic patients is usually higher than that in healthy people. The plasma acetone concentration in healthy people has been reported to be 15±5 μM, whereas in diabetic patients the plasma acetone concentration can reach 1690±780 μM[5]. Exhaled acetone usually ranges from 0.2 to 1.8 ppm in healthy people, and from 1.25 to 2.5 ppm in diabetic patients[6]. Some references show that acetone levels in patients with type 1 diabetes can be as high as 25 ppm[7], thus suggesting that acetone may be a potential biomarker for diabetes. Numerous studies have been conducted

regarding the measurement of acetone in exhaled breath[8,9].

Exhaled breath condensate (EBC) is a liquid sample formed by condensing exhaled breath at low temperatures with the aid of a specialized exhaled breath collection device. EBC is primarily composed of water formed by condensation, but also contains volatile organic compounds (VOCs) as does exhaled breath[10,11]. For example, acetone, which is associated with diabetes[12,13], and propionate, which is associated with asthma-COPD overlap[14], can be found in EBC. There have been many studies reporting the association between biomarkers contained in EBC and lung cancer, inflammation, SARS-CoV-2 (COVID-19), and asthma[15–20]. Monteiro Fernades *et al*. developed plasma optical sensors for the measurement of acetone content in EBC, but no actual EBC measurements have been performed[21]. EBC can be collected frequently and safely, and samples can be obtained quickly and are easier to store and transport than gaseous samples. Several commercially available devices exist that allow for easy and convenient collection of EBC [22] (e.g., RTube). Therefore, the development of facile but reliable EBC sensing devices is expected to provide a more noninvasive and convenient solution for the assessment of lipid metabolism.

There are several methods available for the detection of acetone in aqueous samples. Common methods such as liquid chromatography and selected-ion flow-tube mass spectrometry, can achieve accurate measurement of acetone[23–25], but are costly and complicated to use, making it difficult to meet the needs of clinical and personal health management. Other detection methods, such as colorimetric methods[26], resistive sensor[27–29], cataluminescence sensor[30],ion mobility spectrometry[31], photometric methods[32] and Fourier transform infrared spectroscopy analysis[33], also suffer from long processing time and

insufficient selectivity. The limitations of the existing methods are even more prominent in scenarios that require frequent monitoring or real-time detection, such as the daily management of diabetic patients. For these reasons, we need a portable, fast, and highly sensitive and selective sensor for acetone detection in aqueous samples.

In our previous research, we have developed a biochemical gas sensor, biosniffer, based on an enzymatic reaction, which can measure VOCs including acetone, methanol, ethanol, acetaldehyde, and 2-propanol with high sensitivity and selectivity by detecting changes in fluorescence signals[34–39]. However, the sensor requires a 100-volt AC power source to power the light source, and the large size of the light source and its driver makes it difficult to carry around, limiting its application in clinical and home environments. Therefore, in this study, a handheld battery-powered sensor for acetone detection in aqueous samples was developed, which is small, light in weight, and capable of rapid detection at room temperature to meet the needs of Point-of-Care Testing (POCT) in clinical testing or wearable applications in the future.

Experiment

Reagents and materials

Secondary alcohol dehydrogenase (S-ADH, EC. 1.1.1.x, 1 unit mg^{-1}, product# E001) was bought from Daicel Chiral Technologies (Japan). Hydrophilic polytetrafluoroethylene (H-PTFE) membranes (product# JGWP14225, 80 μm thickness, 80% porosity, 0.2 μm pore size) were bought from Millipore Corporation (USA). β-nicotinamide adenine dinucleotide (NADH) was bought from Oriental Yeast (product# 44326000, Japan). The method of 2-

methacryloyloxyethyl phosphorylcholine polymerized with 2-ethylhexyl methacrylate (PMEH) production was described in a previous study[40,41]. Phosphate buffer (PB) solution was prepared by using potassium dihydrogen phosphate (product# 169-04245, FUJIFILM Wako Chemical, Japan) and disodium hydrogen phosphate (product# 197-02865, FUJIFILM Wako Chemical, Japan). Buffers were made using ultrapure water. Acetone, 2-butanone, 2-pentanone, 2-propanol, acetaldehyde, formaldehyde, 1-propanol, ethanol, nitric Acid, ammonia and methanol were all bought from FUJIFILM Wako Chemical (Japan).

Detection principle of acetone and basic components of the sensor

Fig. 1a shows the principle of an enzymatic reaction based on the measurement of acetone by S-ADH, which catalyzes the reduction of acetone in a slightly acidic environment at pH 6.0-7.0 by oxidizing NADH. NADH fluoresces at 490 nm of wavelength under UV irradiation at 340 nm. The intensity of the fluorescence correlates with the concentration of NADH, and the amount of NADH consumed depends on the concentration of acetone, thus acetone can be detected and quantified by fluorescence measurements.

Based on the above measurement principle, the acetone sensor consists of three basic elements: an enzymatic reaction part, an excitation light source part and a fluorescence measurement part, as shown in Fig. 1b. The enzymatic reaction part consists of a fiber-optic probe (product# SMA(F)/STU 1000-0.04m/SL 1.5(F), Ocean Photonics, Japan) and an S-ADH immobilized enzyme membrane. The S-ADH enzyme membrane was fabricated in the same way as in our prior study[34]. Briefly, after cleaning the hydrophilic PTFE membrane with ultrapure water, the S-ADH solution (100 mg/mL, 10 μL/cm^2) and PMEH solution (10

w/w% in ethanol, 10 μL/cm^2) were mixed and applied to the membrane, which was then dried in a refrigerator at 4 degrees Celsius for 3 h to cure. The excitation light source section consisted of a UV-LED (product# UF4LU-0GD01, DOWA, Japan), an original driver circuit, and a band-pass filter (BPF, product# HMX0340, $\lambda = 340 \pm 5$ nm, Asahi Spectra, Japan). The driver circuit consists of a lithium-ion battery (3.7 V, 2000 mAh, product# DTP605068, DATA POWER TECHNOLOGY, China), a DC/DC converter (product# LTC3111, LINEAR TECHNOLOGY, USA), and a variable current source integrated circuit (product# LT3092EST, Analog Devices, USA). In the excitation light source section, the UV-LED generates ultraviolet light at a wavelength of 340 nm, which serves as the excitation light for NADH. The band-pass filter removes all wavelengths except 340 nm to prevent interference with the experimental measurements. The fluorescence measurement part consisted of a BPF (product# 65-087, 492±5 nm, Edmund Optics, USA) and a photomultiplier tube (PMT, product# H11890-210, Hamamatsu Photonics, Japan), which counts photons based on the received fluorescence signal, converts it into a digital signal and transmits it to a computer. A photograph of the fluorescence detection system is shown in Fig. 1c. The fiber-optic probe in the enzyme reaction part, the UV-LED in the excitation light source section, and the PMT in the fluorescence measurement part were connected by a bifurcated optical fiber (product# SMA(F)/STU 1000-0.04m/SL 1.5(F), Ocean Photonics, Japan).

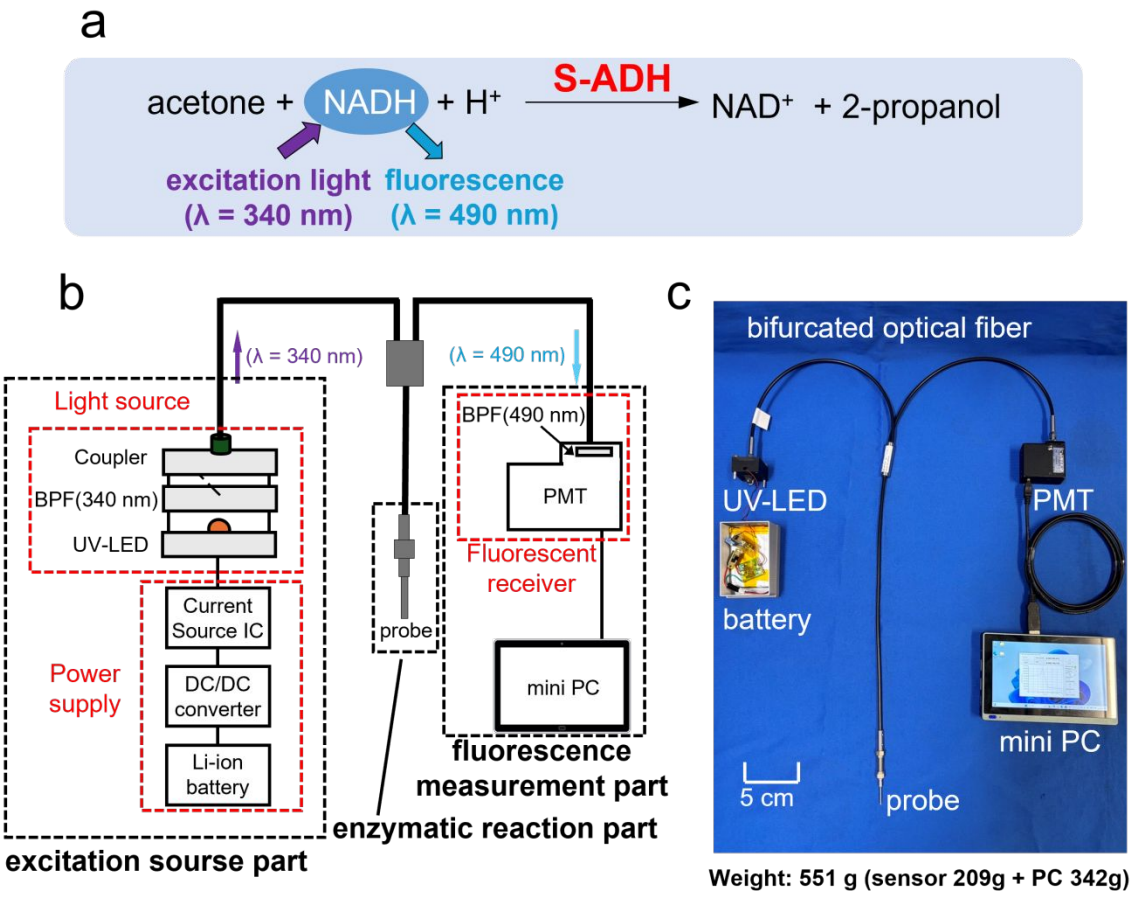

Fig. 1. (a) Principle of acetone detection. (b) Schematic diagram and (c) photo of acetone measurement system.

Sensor optimization including LED light intensity, NADH concentration and selectivity

The light intensity of the UV-LED was varied by changing the value of the current, and the current values required for light intensities at 340 nm from 30 μW to 180 μW were measured and determined using a power meter (product# 7Z01550, Ophir Photonics, Israel). The standard deviation of PMT readings (noise) of the blank solution and average intensity

of 5 μM NADH solution (signal) were measured to calculate the signal-to-noise (SN) ratio. The experiments proceed with different excitation light power to optimize the excitation condition. Also, detection range for NADH concentration was evaluated at optimized excitation light intensity. In the experiment, first, a black-painted cuvette (BRA759116, As One) was filled with PB (pH 8.0, 100 mM, 300 μL), and then fiber-optic probe immersed into it and irradiate the excitation light. Second, NADH solutions were added every 3 minutes to bring the concentration of NADH in the cuvette from 1 nM to 10 mM.

Next, optimum initial NADH concentration for measuring the acetone in aqueous media was evaluated. The concentration of NADH has a significant impact on the enzymatic reaction. Insufficient NADH concentration leads to reduced sensitivity due to inadequate NADH availability for the enzymatic reaction, while excessive NADH concentration results in increased background noise, which is unsuitable for high-sensitivity acetone detection. Therefore, we compared three widely varying concentrations: 5, 50, and 500 μM. In the experiment, NADH was added to PB at different concentrations. The S-ADH-immobilized membrane was fixed to the fiber optic probe using flexible silicone tubing and immersed into NADH solution. Then, acetone solution was added into the cuvette at three-minute intervals to vary the acetone concentration from 10 nM to 10 mM. Note that pH of the buffer and S-ADH amount used for immobilization were same as our previous paper[34].

To assess the selectivity of the sensor, common VOCs in breath and similar VOCs with acetone (2-butanone, 2-pentanone, 2-propanol, acetaldehyde, formaldehyde, 1-propanol, ethanol, and methanol) were measured. The change in fluorescence intensity was measured with S-ADH-immobilized membrane equipped probe by adding each VOCs at 50 μM into

50 μM NADH solution.

Measurement of acetone in EBC

Ten healthy adult participants (7 males and 3 females, aged 21-28 years) participated in the collection of EBC using the RTube (Respiratory Research, USA). The collection device consisted of a large three-way tube (made of polypropylene), which separated saliva from expiration, a one-way valve (made of silicone rubber), and a collection tube that was cooled by a cooling sleeve placed around it. The experiment was planned and conducted in accordance with the Declaration of Helsinki and was approved by the Ethics Committee of the Tokyo Medical and Dental University (approval number: M2020-002). Prior to the experiment, the methods and significance of the study were explained in detail to the participants, and written informed consent was obtained from the participants. All subjects were asked not to drink anything other than water for 2 hours, to avoid exercise for 2 hours before sampling, to refrain from smoking for 72 hours before EBC collection. Also, they rinsed their mouths with water immediately before EBC collection. Prior to taking the sample, a questionnaire was administered to each volunteer asking about basic information including sex, age, body mass index, diet and lifestyle habits. To compare the effect of fasting time on the acetone content of EBC, samples were taken 4 h and 16 h after a meal. The content of the meal was not controlled. During the sampling process, the participants maintained constant breathing for 8 min with an RTube in a sedentary state. Collected EBC samples were stored in a freezer at -80 degrees Celsius after being divided into aliquots. EBC samples thawed back to room temperature before measurement.

Measurements were performed under optimal conditions with a NADH concentration of 50 μM. To avoid NADH dilution effect, 1 μL of 5 mM NADH solution was added to 99 μL of EBC to make an EBC sample containing 50 μM of NADH. Then, 100 μL of the EBC-NADH solution was added to 300 μL of 50 μM NADH solution to measure the acetone concentration.

Results and discussion

Optimal excitation intensity for sensitive measurement of NADH

The SN ratios at different excitation light intensities were evaluated using the NADH fluorescence detection system (see Fig. 2a). The highest SN ratio was observed at an excitation light intensity of 120 μW. This is since a weak light level results in a weaker signal, whereas a strong light level results in too much noise. Fig. 2b shows the increase in fluorescence intensity with increasing NADH concentration from 10 nM to 10 mM with excitation light intensity of 120 μW. The initial fluorescences without NADH was used as a baseline to calculate the sensor output (Δfluorescences) of the sensor. The Δfluorescences was subtract baseline value from fluorescence signal. The relation between fluorescent intensity values and NADH concentration is plotted in Fig. 2c. These plots were fitted using kaleidaGraph software to derive Eq.1.

$$\Delta\text{fluorescences (cps)} = A \times [\text{NADH conc.(nM)}]\text{^}B \qquad \text{Eq.1}$$

Where A = 541.85, B = 0.73

The lower limit of quantification of the fluorescence detection system was calculated to be 20 nM after bringing the 10-fold value of base line standard deviation into Eq.1.

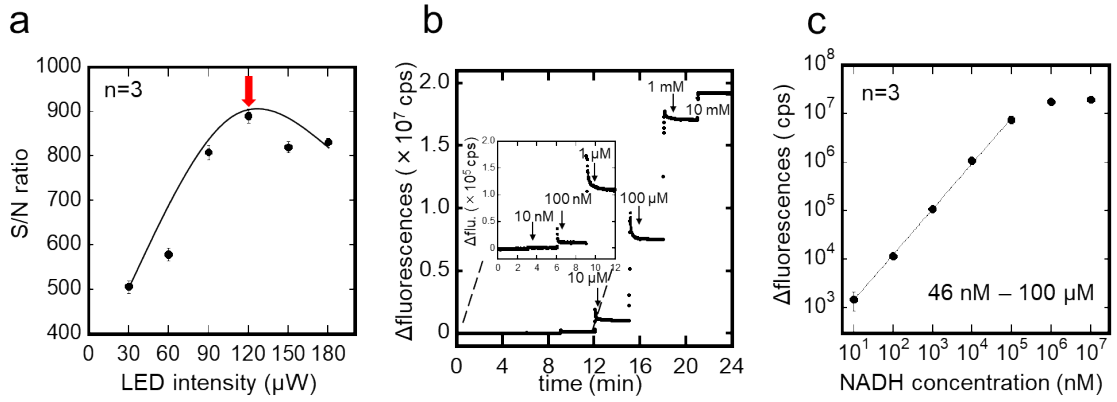

Fig. 2. (a) Comparison of SN ratio under different excitation light intensity. (b) Response curve for NADH measurement. (c) Calibration curve of NADH at 120 μW of excitation light intensity.

Fig. 3a shows an example of the S-ADH biosensor response to a standard acetone solution. As acetone was dripped in, NADH was consumed leading to a decrease in fluorescence intensity. The amount of change in Δfluorescence by adding acetone was defined to ΔF as indicated. Using the initial fluorescence without acetone as a baseline, ΔF were determined from the difference between the baseline and the stable fluorescence observed at different acetone concentrations. The value of ΔF was positively correlated with the acetone concentration. Fig. 3b shows the detection range of the sensor for acetone detection in aqueous samples at different NADH concentrations, with the detection range changing as the NADH concentration changes. In other words, detection ranges of acetone can be controlled by changing the NADH concentration. The acetone concentration in EBC reported about tens of μM and the initial NADH concentration of 50 μM has the lowest coefficient of variation (C.V.) value at 10 μM acetone (see Fig. 3c). Therefore, we chose to

use a 50 μM NADH solution in the EBC detection. To enhance the accuracy of exhaled breath condensate (EBC) measurements, we performed additional quantification of acetone in the range of 1-30 μM, which yielded a linear response. The calibration equation for acetone with 50 μM NADH is shown in Eq. 2.

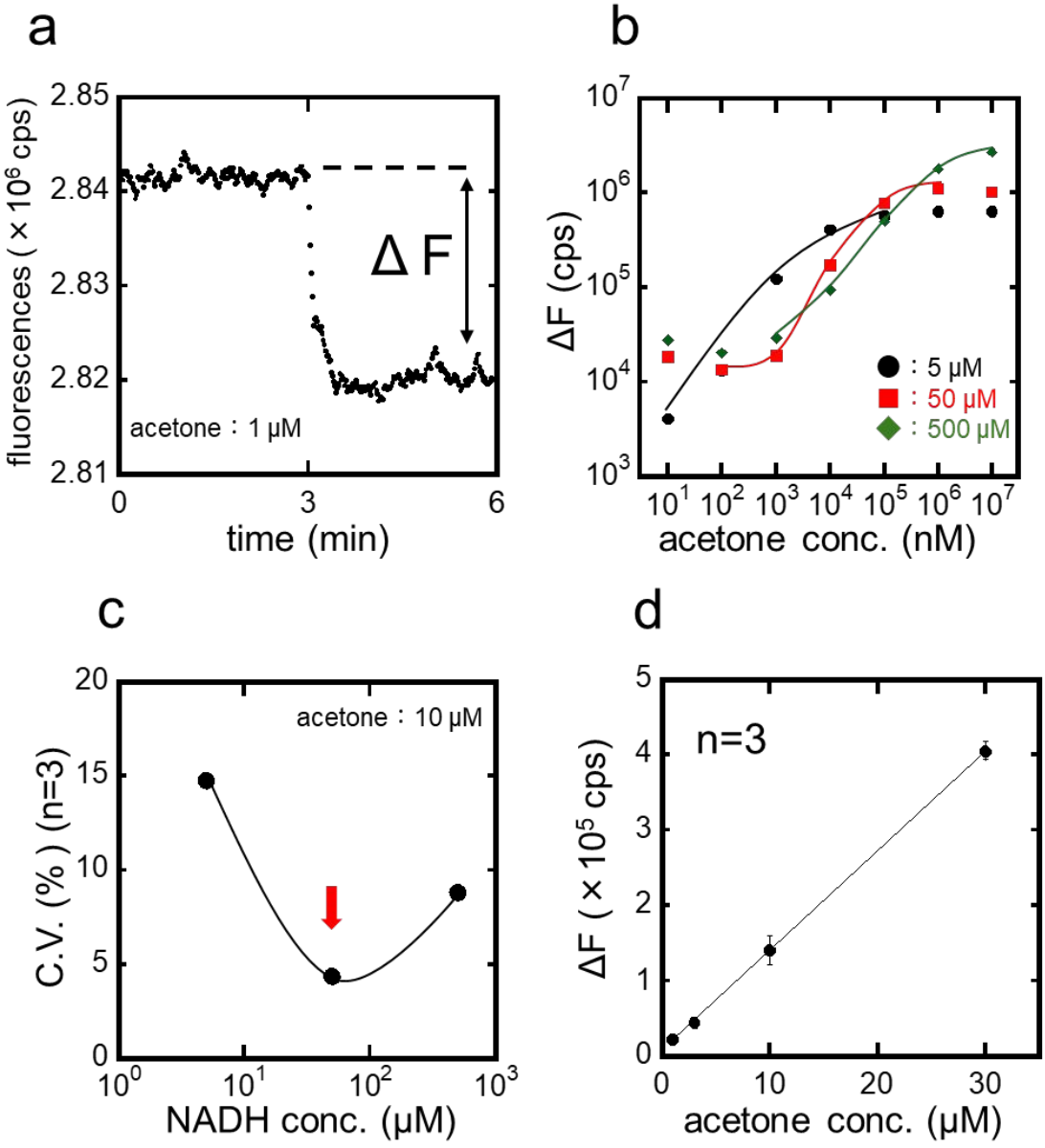

Fig. 3. (a) Sensor responses to 1 μM acetone solution. (b) Detection ranges of acetone

solution at initial NADH concentrations of (●) 5 μM, (■) 50 μM, and (◆) 500 μM (c) C.V in the measurement of 10 μM of acetone for different NADH concentrations (d) The quantification curve for acetone detection when the NADH concentration is maintained at 50 μM.

$$\Delta F\ (cps) = A + B \times [\text{acetone conc. (nM)}] \qquad \text{Eq.2}$$

Where A = 7965.1, B = 13224

The results of the biosensor selectivity evaluation are shown in Fig. 4. The fluorescence intensities of 2-butanol and 2-pentanone were 138% and 111% compared to acetone, respectively, whereas the fluorescence of the other substances was almost undetectable. This indicates that the selectivity of the biosensor depends on the specificity of the S-ADH enzyme. Several studies have shown that 2-butanone and 2-pentanone are present at very low concentrations (nM-levels) in blood and urine and exhaled breath (sub-ppb-levels)[42–44], and therefore their effect can be negligible in acetone measurements in EBC.

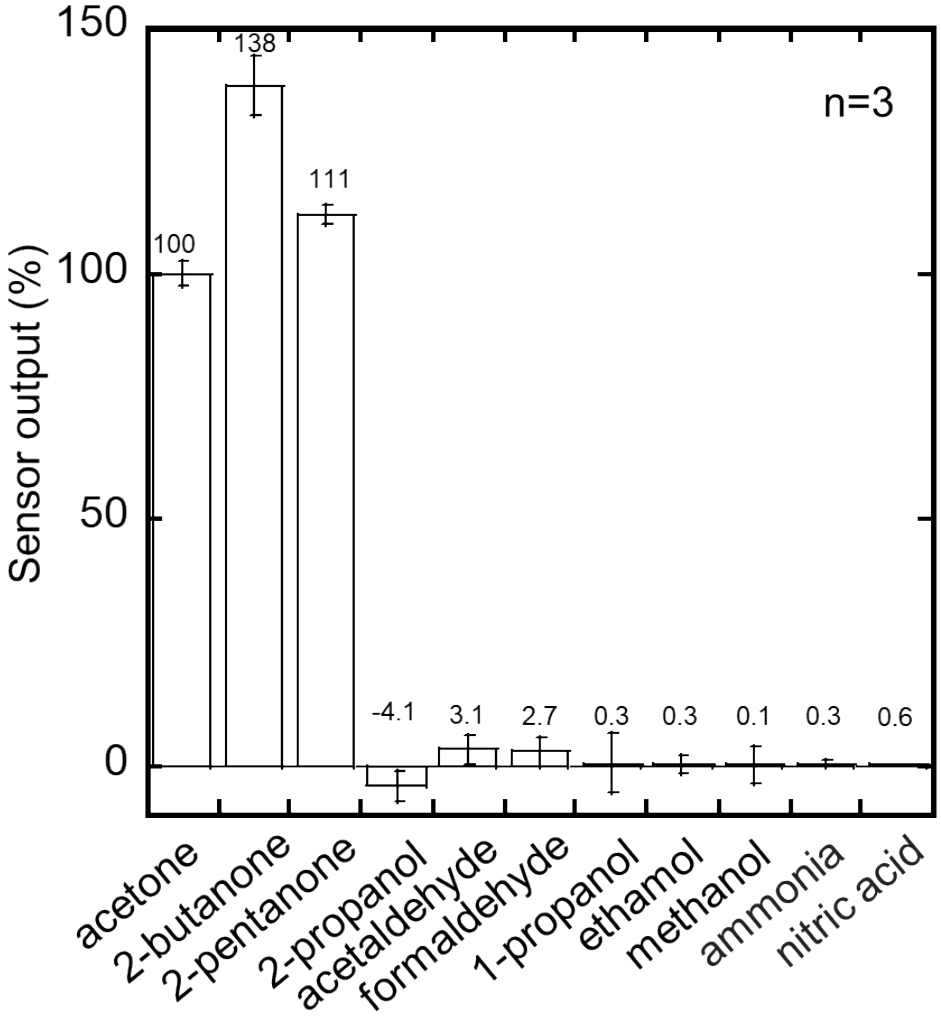

Fig. 4. Relative sensor output to various VOCs solution.

Measurement of acetone in EBC

Fig. 5a shows the process of EBC collection, where the subjects used the RTtube for

8 min after filling out the questionnaire and collected an average of 1.0 to 1.5 mL of EBC. As shown in Fig. 5b, the fluorescence intensity did not change after added 100 μL of a mixture of buffer and NADH, whereas the fluorescence intensity decreased immediately after added a mixture of EBC-NADH solution and reached a steady state within 1 min. The values of fluorescence changes were different between 4 h and 16 h after a meal for the same subject. The concentration of acetone in EBC could be calculated by bringing this fluorescence change value into the quantitative equation for acetone.

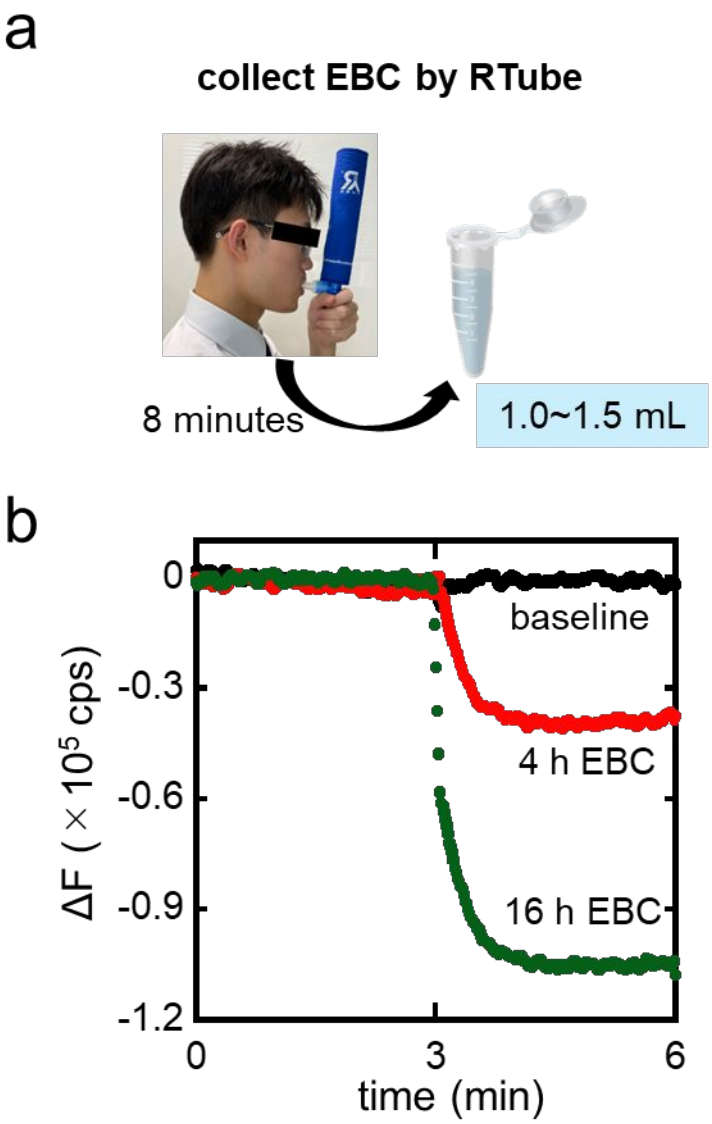

Fig. 5. (a) Procedure for collection of EBC. (b) Sensor responses to NADH solution (baseline) and EBC solution obtained at 4 h and 16 h of fasting.

The measurement results of acetone in EBC are shown in Fig. 6. The average value of acetone content in EBC at 4 h and 16 h after the meal is shown at the top. The concentration of acetone in the 16 h EBC was significantly higher than in the 4 h EBC ($p = 0.011$), Student's

t-test), which is due to the fact that as the fasting time increases, the body begins to break down fat as a source of energy[45]. During lipid catabolism, fatty acids are β-oxidised to produce acetyl coenzyme A. When the rate of production exceeds the utilization capacity of the tricarboxylic acid cycle, the excess acetyl coenzyme A is converted to ketone bodies. As the production of ketone bodies increases, the level of acetone in the blood rises. Acetone in the blood is the most volatile ketone body and enters the alveolar airspace as part of the gas exchange process and is eventually exhaled and dissolved in the EBC. The detection capability of the acetone sensor has been demonstrated with actual samples of EBC.

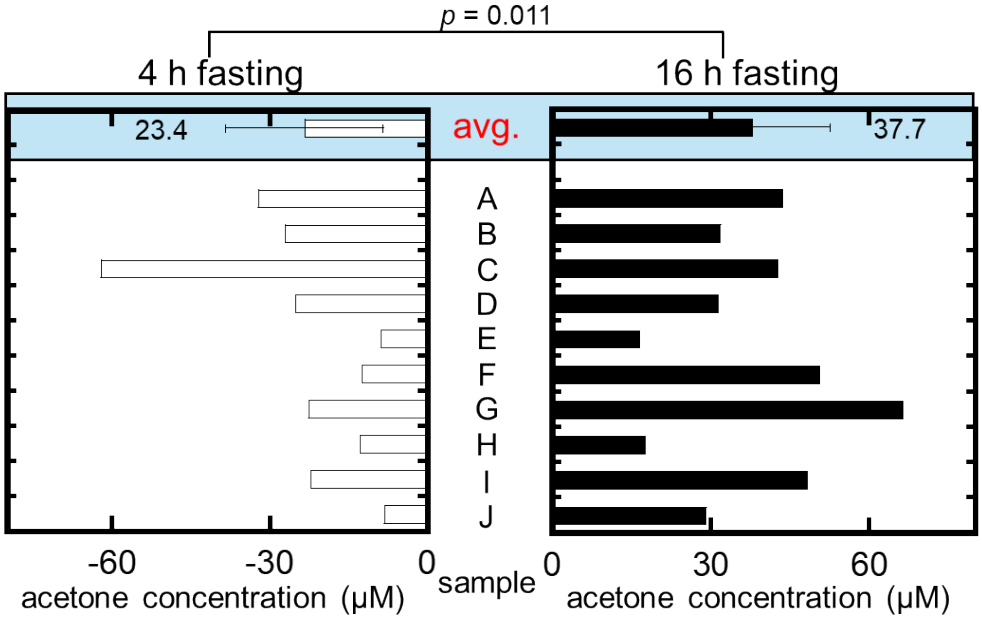

Fig. 6. Comparison of acetone concentration in EBCs at 4 h and 16 h after a meal.

To verify the accuracy of the acetone measurement in the EBC, three samples were selected for the spike and recovery test. The experiment was conducted by configuring an acetone standard solution with the same concentration of acetone as that in the EBC solution,

and then mixing the EBC solution and the standard solution in a 1:1 ratio. The output values of the EBC solution and the mixed solution were compared. The results showed essentially the same output for both solutions with an average recovery of 105% (see Fig. S1).

We further validated the sensor's accuracy through absorbance measurements. The detection principle is analogous to fluorescence detection: during the S-ADH enzyme-catalyzed reduction of acetone, NADH, serving as a coenzyme, is consumed. Since NADH exhibits absorption at 340 nm wavelength, acetone concentration can be determined by measuring the decrease in absorbance. The specific methodology was as follows: An enzyme mixture solution was prepared by dissolving S-ADH in 500 μM NADH solution using pH 6.5 buffer to achieve a final enzyme concentration of 2 mg/mL. The enzyme mixture solution was pipetted into a microplate (product# 3870-096, IWAKI, JAPAN), and baseline absorbance was measured using a microplate reader (product# SH-1000lab, HITACHI, JAPAN). Subsequently, acetone solution was introduced, and the changes in absorbance were measured to derive the quantification equation. Three EBC samples were selected for comparative analysis using this method. The results demonstrated that acetone concentrations determined by both methods were substantially consistent (see Fig. S2). The results of the spike and recovery test and the absorbance measurements demonstrated the accuracy of the acetone biosensor.

Compared to traditional colorimetric methods, our sensor demonstrates enhanced sensitivity. In contrast to high-performance liquid chromatography (HPLC) and ion mobility spectrometry (IMS), our sensor offers superior portability through its handheld design. When compared to photometry and Fourier transform infrared spectroscopy (FTIR) analysis, our

sensor provides simplified operational procedures with minimal sample preprocessing requirements. In comparison with semiconductor chemical sensors, our sensor exhibits higher selectivity for acetone and enables real-time detection at ambient temperature.

Conclusion

We have developed a handheld fluorescent biosensor for the highly sensitive detection of acetone (an indicator of fat metabolism) in aqueous samples. The total weight of the fluorescence detection system was first reduced to 209 g from the original system (5114 g) by using a lithium-ion battery, short optical fibers, and a lab-made compact excitation light driver, making the system handheld. The UV-LED intensity and NADH concentration were then optimized to enable the sensor to detect acetone in the range from 510 nM to 1 mM. The sensor was used to measure the EBC of 10 healthy participants and a significant difference was found between the acetone concentration at 4 h and 16 h of fasting. The measurement results were validated by absorbance measurements and spike and recovery test (recovery rate was 105%). These findings provide not only validation of the sensor's utility, but also a new avenue for metabolic status monitoring. The results of this research contribute to the development of wearable biosensors in the future, which are expected to be widely used in diabetes diagnosis and personal health management.

Supporting information

The supporting information is available free of charge on the XXXXXXX.

Fig.S-1: The response curve of spike and recovery test. (PDF)

Fig.S-2: A comparison between the absorbance detection results and the sensor detection results. (PDF)

Data availability statements

The data supporting this article have been included as part of the Supplementary Information.

Acknowledgments

This work was supported by JST SPRING, Grant Number JPMJSP2120, Japan Society for the Promotion of Science (JSPS) KAKENHI Grant Numbers JP21H04888, JP22K18416, JST ACT-X Grant Number JPMJAX23K2, the Cooperative Research Project of Research Center for Biomedical Engineering.

References:

1 P. Saeedi, I. Petersohn, P. Salpea, B. Malanda, S. Karuranga, N. Unwin, S. Colagiuri, L. Guariguata, A. A. Motala, K. Ogurtsova, J. E. Shaw, D. Bright and R. Williams, *Diabetes Research and Clinical Practice*, 2019, **157**, 107843.

2 Diabetes facts and figures show the growing global burden for individuals, families, and countries. The IDF Diabetes Atlas (2021) reports that 10.5% of the adult population (20-79 years) has diabetes, with almost half unaware that they are living with the condition., https://idf.org/about-diabetes/diabetes-facts-figures/, (accessed August 8, 2024).

3 L. Weiss, P. Reix, H. Mosnier-Pudar, O. Ronsin, J. Beltrand, Q. Reynaud, L. Mely, P.-R. Burgel, N. Stremler, L. Rakotoarisoa, A. Galderisi, K. Perge, N. Bendelac, M. Abely and L. Kessler, *Diabetes & Metabolism*, 2023, **49**, 101444.

4 S. Das, S. Pal and M. Mitra, *J. Med. Biol. Eng.*, 2016, **36**, 605–624.

5 M. P. Kalapos, *Biochimica et Biophysica Acta (BBA) - General Subjects*, 2003, **1621**, 122–139.

6 A. Rydosz, *J Diabetes Sci Technol*, 2015, **9**, 881–884.

7 A. Rydosz, *Sensors*, 2018, **18**, 2298.

8 A. Verma, D. Yadav, S. Natesan, M. Gupta, B. Chandra Yadav and Y. Kumar Mishra, *Microchemical Journal*, 2024, **201**, 110713.

9 A. Verma, D. Yadav, A. Singh, M. Gupta, K. B. Thapa and B. C. Yadav, *Sensors and Actuators B: Chemical*, 2022, **361**, 131708.

10 M. A. G. Wallace and J. D. Pleil, *Analytica Chimica Acta*, 2018, **1024**, 18–38.

11 S. Dodig and I. Čepelak, *Biochem Med*, 2013, 281–295.

12 S. Szunerits, H. Dörfler, Q. Pagneux, J. Daniel, S. Wadekar, E. Woitrain, D. Ladage, D. Montaigne and R. Boukherroub, *Anal Bioanal Chem*, 2023, **415**, 27–34.

13 C. P. Costa, J. Marques, D. Silva, C. Barbosa, A. S. Oliveira, M. Santos and S. M. Rocha, *Microchemical Journal*, 2021, **171**, 106830.

14 N. Ghosh, P. Choudhury, M. Joshi, P. Bhattacharyya, S. Roychowdhury, R. Banerjee and K. Chaudhury, *Sci Rep*, 2021, **11**, 16664.

15 J. Połomska, K. Bar and B. Sozańska, *JCM*, 2021, **10**, 2697.

16 G. Bang, J. H. Park, C. Park, K. Kim, J. K. Kim, S. Y. Lee, J. Y. Kim and Y. H. Park, *J Anal Sci Technol*, 2022, **13**, 37.

17 M. Seifi, N. Rastkari, M. S. Hassanvand, K. Naddafi, R. Nabizadeh, S. Nazmara, H. Kashani, A. Zare, Z. Pourpak, S. Y. Hashemi and M. Yunesian, *Sci Rep*, 2021, **11**, 12922.

18 A. Gholizadeh, K. Black, H. Kipen, R. Laumbach, A. Gow, C. Weisel and M. Javanmard, *RSC Adv.*, 2022, **12**, 35627–35638.

19 E. Barberis, E. Amede, S. Khoso, L. Castello, P. P. Sainaghi, M. Bellan, P. E. Balbo, G. Patti, D. Brustia, M. Giordano, R. Rolla, A. Chiocchetti, G. Romani, M. Manfredi and R. Vaschetto, *Metabolites*, 2021, **11**, 847.

20 S. Kazani, A. Planaguma, E. Ono, M. Bonini, M. Zahid, G. Marigowda, M. E. Wechsler, B. D. Levy and E. Israel, *Journal of Allergy and Clinical Immunology*, 2013, **132**, 547–553.

21 G. B. Monteiro Fernandes, H. Nascimento, R. M. Santa Cruz, J. L. Brum Marques and C.

Da Silva Moreira, *Plasmonics*, DOI:10.1007/s11468-023-02190-4.
22 E. M. Konstantinidi, A. S. Lappas, A. S. Tzortzi and P. K. Behrakis, *The Scientific World Journal*, 2015, **2015**, 435160.
23 S. Fujii, T. Maeda, I. Noge, Y. Kitagawa, K. Todoroki, K. Inoue, J. Z. Min and T. Toyo'oka, *Clinica Chimica Acta*, 2014, **430**, 140–144.
24 T. Wang, P. Španěl and D. Smith, *International Journal of Mass Spectrometry*, 2008, **272**, 78–85.
25 H. Kim and H. Shin, *J of Separation Science*, 2011, **34**, 693–699.
26 J. Liang, H. Li, J. Wang, H. Yu and Y. He, *Anal. Chem.*, 2020, **92**, 6548–6554.
27 C. Felice, G. Lein, K. S. V. Santhanam and L. Fuller, *Mat Express*, 2011, **1**, 219–224.
28 M. Gupta, P. Chaudhary, A. Singh, A. Verma, D. Yadav and B. C. Yadav, *Sensors and Actuators B: Chemical*, 2022, **368**, 132102.
29 M. Gupta, A. Verma, P. Chaudhary and B. C. Yadav, *ACS Appl. Electron. Mater.*, 2024, acsaelm.4c00571.
30 P. Yang, C. Lau, X. Liu and J. Lu, *Anal. Chem.*, 2007, **79**, 8476–8485.
31 R. Garrido-Delgado, L. Arce, C. C. Pérez-Marín and M. Valcárcel, *Talanta*, 2009, **78**, 863–868.
32 N. Teshima, J. Li, K. Toda and P. K. Dasgupta, *Analytica Chimica Acta*, 2005, **535**, 189–199.
33 S. G. A. van der Drift, R. Jorritsma, J. T. Schonewille, H. M. Knijn and J. A. Stegeman, *J Dairy Sci*, 2012, **95**, 4886–4898.
34 M. Ye, T. Arakawa, P.-J. Chien, T. Suzuki, K. Toma and K. Mitsubayashi, *IEEE Sensors J.*, 2017, **17**, 5419–5425.
35 K. Toma, K. Iwasaki, T. Arakawa, Y. Iwasaki and K. Mitsubayashi, *Biosensors and Bioelectronics*, 2021, **181**, 113136.
36 H. Kudo, M. Sawai, X. Wang, T. Gessei, T. Koshida, K. Miyajima, H. Saito and K. Mitsubayashi, *Sensors and Actuators B: Chemical*, 2009, **141**, 20–25.
37 K. Iitani, P.-J. Chien, T. Suzuki, K. Toma, T. Arakawa, Y. Iwasaki and K. Mitsubayashi, *ACS Sens.*, 2017, **2**, 940–946.
38 G. Zhang, Y. Maeno, K. Iitani, T. Arakawa, Y. Iwasaki, K. Toma and K. Mitsubayashi, *Sensors and Actuators B: Chemical*, 2024, **401**, 135031.
39 P.-J. Chien, M. Ye, T. Suzuki, K. Toma, T. Arakawa, Y. Iwasaki and K. Mitsubayashi, *Talanta*, 2016, **159**, 418–424.
40 M. Chu, H. Kudo, T. Shirai, K. Miyajima, H. Saito, N. Morimoto, K. Yano, Y. Iwasaki, K. Akiyoshi and K. Mitsubayashi, *Biomed Microdevices*, 2009, **11**, 837–842.
41 K. Ishihara, S. Tanaka, N. Furukawa, N. Nakabayashi and K. Kurita, *J. Biomed. Mater. Res.*, 1996, **32**, 391–399.
42 T. Kawai, Z.-W. Zhang, A. Takeuchi, Y. Miyama, K. Sakamoto, K. Higashikawa and M. Ikeda, *Int Arch Occup Environ Health*, 2003, **76**, 17–23.
43 S. K. Pandey and K.-H. Kim, *TrAC Trends in Analytical Chemistry*, 2011, **30**, 784–796.
44 B. De Lacy Costello, A. Amann, H. Al-Kateb, C. Flynn, W. Filipiak, T. Khalid, D. Osborne and N. M. Ratcliffe, *J. Breath Res.*, 2014, **8**, 014001.
45 F. Bovey, J. Cros, B. Tuzson, K. Seyssel, P. Schneiter, L. Emmenegger and L. Tappy, *Nutr & Diabetes*, 2018, **8**, 50.

The data supporting this article have been included as part of the Supplementary Information.